Theor Chem Acc (2011) 130:563–570
DOI 10.1007/s00214-011-1061-2

REGULAR ARTICLE

Theoretical study of the V(^4F) + NO($^2\Pi_r$) → VO($^4\Sigma^-$) + N($^4S°$) reaction compared with the Sc(^2D) and Ti(^3F) cases

Dong-ki Lee · Young Choon Park · Yoon Sup Lee · Gwang-Hi Jeung

Received: 8 March 2011 / Accepted: 30 September 2011 / Published online: 18 October 2011

Abstract To understand the title reaction, the MRCI, CCSD, CCSD(T), and DFT calculations have been done. A large domain of the ground-state potential energy surface has been explored including the activation energy barrier to form the triatomic complex, two stable intermediate complexes, V[NO] and NVO, the transition state connecting these two conformers, and the detachment of the nitrogen atom. We compared this reaction with the similar ones involving the Sc and Ti atoms. The activation barrier to form the VNO complex made from the ionic-covalent coupling decreases to approach the experimental data when the electron correlation effect is better included as in the Sc and Ti systems. The transition state connecting the two conformers was calculated to be higher than in the Sc and Ti cases probably due to larger number of nonbonding valence electrons and is probably too high with respect to the reactant energy level to allow the interconversion between the two conformers in the VNO. The direct concerted substitution (abstraction) reaction is improbable because this process will have to overcome a too high potential barrier. We have also found the transition state connecting two conformers of ScNO.

Keywords Reaction potential surface · Conformers · Transition states · Electron correlations · Ionic-covalent coupling

1 Introduction

The electron transfer occurs in the first step of the oxidation reaction of the metal atom with an oxidant molecule. As a metal atom and an oxidant like O_2, NO, etc., come in close contact in the first course of collision, the initial repulsive covalent configuration meets an attractive ionic configuration. If the energy barrier formed by the coupling between these two configurations is lower than the reactant energy, then a metal–ligand complex can be formed due to the Coulomb force. A given metal–ligand complex has in general many stable conformers on the potential energy surface (PES). To understand the mechanism of obtaining the metal monoxide as final product, a good knowledge about the metal–ligand intermediate conformers and the transition state is required.

We have recently studied the reaction potential surfaces of the Al + O_2 [1], Sc + NO and Sc + O_2 [2], and Ti + NO and Ti + O_2 [3] systems. These reactions have been studied by various experimental techniques (see the references therein). The activation barriers for those reactions were calculated using high-level quantum chemical methods, which appeared to overestimate those barriers in comparison with the known experimental data. For the Al + O_2 → AlO + O reaction, the calculated reaction barrier height was 0.11 eV [1] while the experimental data indicated less than 0.006 eV [4]. In contrast, the calculated reaction enthalpy −0.07 eV [1] was in fairly good agreement with the experimental value −0.155 eV [4]. In the Sc + NO → ScO + N reaction, the low-level calculation

---

Dedicated to Professor Shigeru Nagase on the occasion of his 65th birthday and published as part of the Nagase Festschrift Issue.

D. Lee · Y. C. Park · Y. S. Lee (✉)
Department of Chemistry, Korea Advanced Institute of Science and Technology (KAIST), 305-701 Daejeon, Korea
e-mail: Yslee@kaist.edu

G.-H. Jeung
Chimie Théorique, Case 521 (CNRS-UMR-6224),
Université d'Aix-Marseille, Campus de Saint-Jérôme,
13397 Marseille Cedex 20, France
e-mail: Jeung@up.univ-mrs.fr

(CASSCF) gave 0.17 eV and the high-level calculation (MRCI) gave 0.19 eV [2] versus the experimental value 0.10 eV [5, 6]. For the Ti + O → TiO + O reaction, the CASSCF gave 0.47 eV and the MRCI gave 0.52 eV [3] versus the experimental value 0.110 eV [7, 8]. The density functional theory (DFT) has also been used for these reactions, but the reaction barrier calculated with various functionals did not give consistently reliable results, either. The activation barrier made from a subtle ionic-covalent coupling is quite difficult to calculate accurately, and describing the ionic-covalent coupling in a well-balanced way is a challenging problem of quantum chemistry.

Another important aspect is related to the existence of three conformers for the metal oxidant complexes MNO and MO_2. All three conformers were found in all complexes we have studied so far, AlO_2, ScNO, ScO_2, TiNO, and TiO_2. In these cases, the triangular NMO conformer with an obtuse $\angle$(NMO) angle is lower in energy than the other triangular conformer represented as M[NO] with an acute $\angle$(NMO) angle. It is noted that the trend is same for the all MO_2 complexes hereafter. Both conformers are lower in energy than the linear MNO complex. The linear MNO conformer is separated from the triangular M[NO] conformer by a transition state (TS1), and the triangular M[NO] conformer is separated from the triangular NMO conformer by another transition state (TS2). However, the energy level of TS1 is significantly lower than the reactant energy, and the linear MNO conformer does not have deep enough potential well around. As a consequence, the linear conformer cannot survive long enough before being transformed to the triangular M[NO] conformer. In contrast, TS2 has a relatively high energy in comparison with the energy levels of the two triangular conformers; thus, these two conformers can have relatively long life time depending upon the energy level of TS2. The TiNO and TiO_2 complexes have TS2 lying lower than the reactant energy [3], while TS2 in the Sc cases could not be located at the time [2]. The M[NO] conformer is connected with the reactant state by an activation barrier. The product state is connected with the NMO conformer without any potential barrier in the Sc and Ti cases. However, there is no energetically accessible reaction path between the reactant state and the NMO conformer, nor between the product state and the M[NO] conformer. The transition state between the two conformers retains a key role in the formation of the metal monoxides.

In this work, we have studied an oxidation reaction involving the vanadium atom in the ground state, $V(^4F) + NO(X^2\Pi_r) \rightarrow VNO \rightarrow VO\ \ (X^4\Sigma^-) + N\ \ (^4S°)$. This reaction has been recently studied by Ishida et al. using a crossed beam technique [9]. They have observed the VO product, and its statistical rotational distribution made them to conclude the existence of a long-living VNO intermediate. The activation barrier was estimated to be 8.4 kJ mol^{-1} (0.087 eV). The aims of this work are to test the reliability of the high-level *ab intio* method to estimate the reaction barrier on one hand and to find the transition states among the three conformers and compare those with Sc and Ti cases on the other hand. Toward that end, we survey a large area of the ground-state PESs and analyze the wavefunctions at several important geometrical points. In this work, we also give new results on the $Sc(^2D) + NO(^2\Pi_r) \rightarrow ScO(^2\Sigma^+) + N(^4S°)$ reaction, including a newly located TS2 not available in our previous work [2].

2 Method of computation

The complete active space (CAS), self-consistent field (SCF) calculation, and the multi-reference (MR) configuration interaction (CI) were done using the Molcas [10] program. The Hartree–Fock (HF) and the coupled cluster (CC) method were done using the Molpro [11] and the Gaussian [12] programs. The density functional theory (DFT) calculation was done using the Gaussian program. Extended atomic basis sets were optimized to describe simultaneously the covalent and ionic configurations. The Gaussian-type orbitals (GTOs) used consist of 16s11p7d2f for V atom and 12s7p3d for N and O atoms. These GTOs were contracted to 12s9p5d2f for V and 8s5p3d for N and O atoms to make the atomic basis functions (ABFs). For the CAS-SCF, 12 active electrons and ten molecular orbitals (MOs) were used with the C_{2v} (for linear geometry) or the C_s (for triangular geometry) point-group symmetry. The reactants can make the triplet, quintet, and septet spin symmetries. The MRCI used slightly reduced active space from the CAS-SCF and included, e.g. from 1,969,279 configuration state functions (CSFs) for the $^7A'$ state or 6,906,288 CSFs for the $^5\Delta$ state to 9,990,590 CSFs for the $^5A'$ state. The geometry and the corresponding energy of local minima (intermediate complex in different conformers) were located by interpolating the PES.

For the coupled-cluster singles and doubles (CCSD) and the singles and doubles with noniterative triples (CCSD(T)) calculations, the same basis set was used and 4 s and 3d electrons of the V atom and 2p electrons of N and O atoms were correlated. The critical points (geometries), i.e. the local minima (intermediate complex in different conformers) and the local maxima (transition states), were located by the geometry optimization at the CCSD level, and the resulting geometries were used for the CCSD(T) calculations. The B3LYP functional [13] was adopted for the DFT calculations using the same basis set we have optimized for the MRCI. The vibrational frequencies were calculated using the gradient subroutines. The effective point charges of the three atoms for the triangular geometry were calculated from two components of the dipole moment together with the condition that the sum of the effective charges should vanish.

It is useful to check the accuracy of the computational method for the reactant and product states. We have done a small MRCI calculation for the VO molecule with 105,198 CSFs. For the ground state of VO($^4\Sigma^-$), we have obtained $R_e = 157.5$ pm, $D_e = 6.069$ eV, $D_0 = 6.008$ eV, $\omega_e = 1{,}075$ cm^{-1}, $\omega_e x_e = 4.1$ cm^{-1}, and the dipole moment $\mu_e = 1.191$ a.u. (effective charge: 0.397 a.u.). The available experimental data [14] show $R_e = 158.93$ pm, $\omega_e = 1{,}011.3$ cm^{-1}, and $\omega_e x_e = 4.86$ cm^{-1}, which are quite close to the calculated values. There is a gas phase data for the D_0 estimated to be 6.458 eV [15], but its accuracy is in question. The equilibrium NO distance in VNO with a very large distance between the vanadium atom and the nitric oxide was calculated to be 114 pm in the MRCI, which is close to the experimental value, 115.077 pm. The bond distance and the harmonic vibration frequency of VO calculated in CCSD are, respectively, 159.7 pm and 983 cm^{-1}. The DFT calculation gave 158.3 pm and 1,039 cm^{-1}.

The triplet and septet states of VNO proved to be much higher in energy in comparison with the quintet states for the compact geometries. Since the A′ state participates in the bond formation and breaking in this reaction, we concentrate on the ^{5}A′ state in the triangular geometries, or the $^5\Delta$ state for linear geometries. Ideally, it would be better to treat the V(^{4}F) + NO($^2\Pi_r$) → VNO → VO($^4\Sigma^-$) + N(^{4}S°) reaction in a single scheme using only the C_s point-group and keeping the same active space in CAS-SCF and MRCI all along. As this is impractical, we have studied this reaction in two parts, V(^{4}F) + NO($^2\Pi_r$) → VNO(^{5}A′) and VNO(^{5}A′) → VO($^4\Sigma^-$) + N(^{4}S°). As was mentioned in the previous section, we found that the intermediate complex, VNO, can exist in two stable triangular conformers V[NO] and NVO. The title reaction can be further divided into three consecutive steps depending upon whether the title reaction is concerted or not in reality as

(Step 1) V(^{4}F) + NO($^2\Pi_r$) → V[NO](^{5}A′)
(Step 2) V[NO](^{5}A′) → NVO(^{5}A′)
(Step 3) NVO(^{5}A′) → VO($^4\Sigma^-$) + N(^{4}S°).

We are going to discuss the reaction following this consecutive sequence. The potential energy levels minima (conformers) and maxima (transitions states) involved in this reaction are schematically drawn in Fig. 1 using the energy levels found in the CCSD(T) calculations.

3 Results and discussion

3.1 *Step 1* V(^{4}F) + NO($^2\Pi_r$) → V[NO](^{5}A′)

In Step 1, as the distance between the vanadium atom and the nitric oxide decreases in the course of collision, the potential energy increases due to the repulsion between the electronic spatial extension of the metal atom and that of the NO molecule. The nitric oxide is known to have a small electron affinity, 0.026 eV, from a photodetachment experiment [16]. However, when coordinated to a metal atom, there occurs the electron transfer from the metal atom to NO at relatively short intermolecular distances, e.g. around R(V–N) = 4.7 bohr for V–NO collinear collision, so the potential energy decreases for more compact geometry due to the Coulomb force. The transition state is made from a coupling between the repulsive covalent configuration and the attractive ionic configuration. We found that the collinear approach with the nitrogen atom colliding with the metal atom, thus forming VNO linear form, is energetically the lowest in comparison with other approaches, namely the VON collinear form or the side-on (the atoms making a triangular form with N–O distance close to the free NO value) form. The side-on approach is the next lowest, and the VON collinear approach is energetically the highest, although all approaches lead to the attractive potential well once the activation energy is overcome. The rotating NO molecule would get aligned preferentially to confirm the VNO collinear form during Step 1, transferring the rotational energy to the complex.

The ionic-covalent coupling regions are usually very hard to describe in quantum chemical methods. The ionic configuration and the covalent configuration are very different and so are their electron correlation effects. One section of PES for Step1, keeping the N–O distance fixed at 2.2 bohr, is reported in Fig. 2 where the MRCI-1 is one-state calculation and MRCI-2 is two-state calculation. In looking at the CAS-SCF, the MRCI-1, then the MRCI-2 curves, one can see the effect of the electron correlation that strongly lowers the activation barrier from 1.17 eV in CAS-SCF to 0.87 eV in MRCI-1 and at the same time relocates the transition state to a larger intermolecular distance. A more balanced description of the electron correlation effect for both ionic and covalent configurations by calculating the two states simultaneously at the CAS-SCF level to obtain the average MOs makes actually the ionic configuration more accessible in comparison with the covalent configuration for this particular case, reduces the activation barrier further from 0.87 eV in MRCI-1 to 0.48 eV in MRCI-2, and at the same time shifts the transition state to still a larger intermolecular distance. The origin of this can be traced back to the ionic asymptote with respect to the covalent asymptote discussed recently

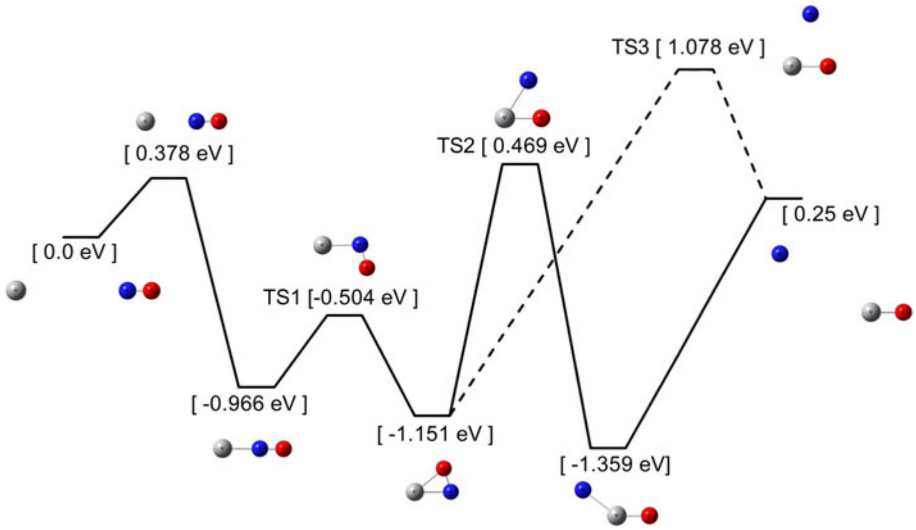

Fig. 1 Schematic diagram of the energy levels and the molecular geometries of the minima (conformers) and maxima (transition states) involved in the title reaction. The numbers are taken from the CCSD(T) calculation. Vanadium atom is *colored* in *gray*, nitrogen atom in *blue*, and oxygen atom in *red*

[17, 18]. In general, the molecular calculation overestimates the energy level of the ionic asymptote in comparison with the covalent asymptote when the basis set is not large enough or when the electron correlation effect is not sufficiently taken into account. Thus, Fig. 2 shows the importance of choosing an appropriate active space (set of MOs where the active electrons are distributed in all possible way) to obtain more realistic result. Table 1 reports the activation barrier for Step 1 of the title reaction. We can see there that the methods used in this work consistently overestimate the activation barrier (AB) in comparison with the experimental value, 0.087 eV [9]. We expect this barrier to be lowered to match the experimental value if the electron correlation effect is taken into account much more extensively, e.g. by a larger scale MRCI. In contrast, the DFT calculation using the B3LYP functional did not give any activation barrier, which is contrary to the experimental observations.

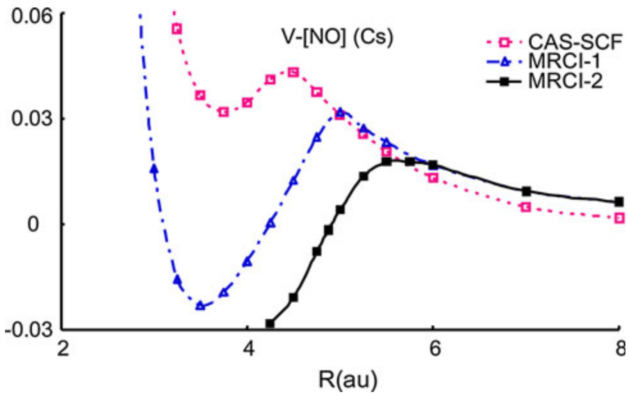

Fig. 2 One C_s section of potential energy surfaces of VNO for Step 1. The N–O distance (r) is fixed to 2.2 bohr along the side-on geometry, i.e. the Jacobian angle (θ) is $\pi/2$, and R in bohr is the distance between V and the mid-point between the N and O atoms. See text for different curves

In Fig. 3 is drawn a section of PES where the $\phi = \angle$NVO angle is varied from 0° to 180°. For each angle, the lowest energy calculated in MRCI is reported in this figure. Here, we can see the potential well corresponding to all three conformers and two transition states separating them. When $\phi = 0°$, the lowest energy is found for the linear VNO. For $\phi = 180°$, the lowest energy is found in the linear NVO, but it is not a local minimum. Once the activation barrier is overcome, the attractive potential leads to the linear VNO conformer. However, the triangular V[NO] conformer is significantly lower in energy than the linear VNO one, and TS1 separating these two conformers is not high enough. The probability of finding the triangular V[NO] at any given time would be much higher than that of finding the linear VNO. Both CCSD and DFT methods also confirmed the existence of TS1 with its energy level significantly lower than the reactant energy level.

3.2 *Step 2* V[NO]($^5A'$) → NVO($^5A'$)

Two different sections of PES are superposed in Fig. 4. One section concerns varying the $\angle$VNO angle (θ) with R(V–N) = 3.67 bohr and R(N–O) = 2.26 bohr (in solid curve). $\theta = 180°$ corresponds to the linear VNO. Reminding that the collinear V–NO collision was energetically the lowest, we can see that once the activation barrier through the collinear collision is overcome, the potential decreases until a triangular geometry with an obtuse $\angle$VNO angle is formed. Then, we can see a low potential barrier under the reactant energy level when this angle becomes smaller. The reactant energy is large enough to easily get over this barrier then the V[NO] conformer with an acute $\angle$VNO angle would be made. The second section concerns varying the $\angle$VON angle (θ) with R(V–O) = 3.67 bohr and R(N–O) = 2.26 bohr (in broken curve). Reminding that the collinear V–ON collision passes

Table 1 Calculated activation energy (AE) and the geometrical parameters of the linear VNO transition state in Step 1

	MRCI	CCSD(T)	CCSD	DFT	Exp.[a]
AE/eV	0.410	0.378	0.405	none	0.087[a]
R(V–N)/pm	249	CCSD	259		
R(N–O)/pm	120	CCSD	114		

[a] From [7]

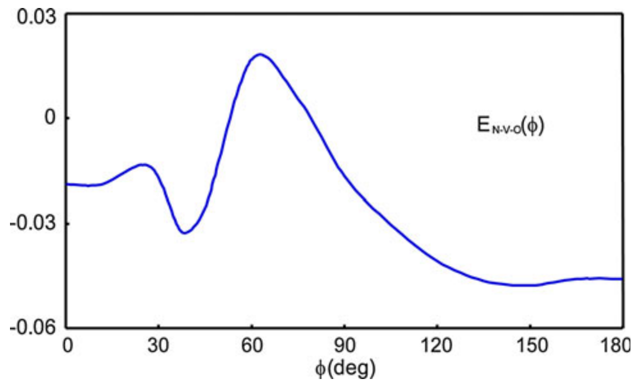

Fig. 3 A section of the ground-state potential energy surface (with respect to that of the reactant, V + NO) following the lowest potential for given ϕ (∠NVO), 0° corresponds to the linear VNO geometry, and 180° corresponds to the linear NVO geometry

through the highest activation barrier, we see that the energy decreases monotonically once the activation barrier is overcome and the V[NO] conformer with an acute ∠VNO angle would be made as the ∠VON angle is decreased. In any case, the first intermediate complex would be the V[NO] conformer.

Fig. 3 also shows TS2 separating the two triangular conformers. The characteristics of these conformers are resumed in Table 2. In V[NO], the R(V–N) distance is slightly smaller than the R(V–O) distance, and the R(N–O) distance is slightly enlarged compared with that of the free NO. In this conformer, the metal atom transfers about 0.30 electrons to the NO moiety that is mostly localized at the nitrogen atom. So, we can regard this complex made from a bonding between the metal atom and the NO molecule via a partial electron transfer to the π open-shell of NO. Here, the N–O bond is mostly intact. R(V–O) in the triangular NVO conformer is slightly larger than that of the free VO molecule, while R(V–N) is much larger than R(V–O). R(N–O) = 357 pm is more than three times that of the free NO. In this triangular NVO conformer, the metal atom cedes about 0.73 electrons to the oxygen atom and 0.64 electrons to the nitrogen atom. We may regard this conformer made with two ionic bonds, V–O and V–N, without any N–O bonding.

The three vibrational frequencies of the VNO complex calculated with the CCSD and the DFT methods are listed in Table 2. The highest vibrational frequency (ν_3) of the V[NO] conformer, 1,236 cm^{-1} (CCSD) or 1,237 cm^{-1} (DFT), is much smaller than the harmonic frequency (ω_e) of the free NO, 1,904 cm^{-1} [14, 19] confirming that the N–O bond is significantly weakened upon coordination to the metal atom.

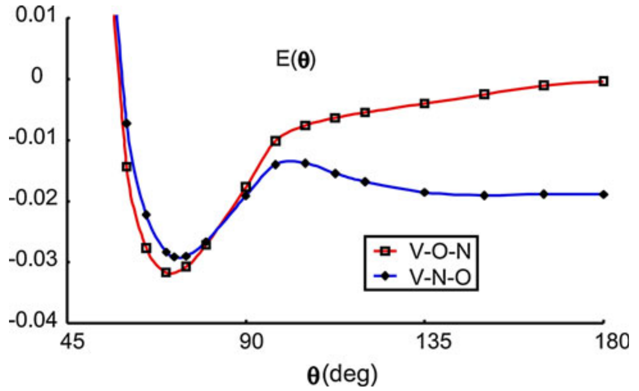

Fig. 4 Superposition of two different sections of the ground-state potential energy surface (energies with respect to that of the reactant, V + NO). For the *blue curve*, θ represents the ∠VNO angle, R(V–N) = 3.67 bohr and R(N–O) = 2.26 bohr. For the *red curve*, θ represents the ∠VON angle, R(V–O) = 3.67 bohr and R(N–O) = 2.26 bohr

The energy level of TS2 and the corresponding geometry calculated in different methods are reported in Table 3. The potential barrier separating these two conformers culminated by TS2 was calculated to be higher than the initial reactant energy level in all methods, MRCI, CCSD(T), CCSD, and DFT. This is in contrast to the TiNO, TiO_2, and ScNO cases where the TS2 is significantly lower than the reactant energy level. We think that the problem again is in the unbalanced description of the two lowest potential energy surfaces as in the activation barrier (AB) case. As the vanadium complex include one or two more valence electron than the Ti and Sc complexes, a large-scale correlated calculation for the vanadium case may lower TS2. However, we cannot specify any definite order for the relative energy levels between the collision energy and TS2 from the current result.

3.3 *Step 3* NVO($^5A'$) → VO($^4\Sigma^-$) + N($^4S°$)

The last step of the title reaction is the detachment of nitrogen atom. In principle, this can be done from either conformer, from the triangular V[NO] conformer or from the triangular NVO conformer. The former implies simultaneously breaking two bonds, V–N and O–N, which is expected to be energetically costly as shown in Fig. 1 for the CCSD(T) calculation. In contrast, breaking the single V–N bond from the triangular NVO conformer occurs without any potential barrier in all methods of calculation, MRCI, CCSD(T), CCSD, and DFT. Yet another possibility

Table 2 Binding energy (BE, with respect to V + NO), geometrical parameters, effective charges, and the vibrational frequencies (ν) of the V[NO] and NVO conformers (Step 2)

Method	V[NO]	NVO
BE/eV		
MRCI	0.886	1.302
CCSD(T)	1.151	1.359
CCSD	0.887	1.095
DFT	1.869	1.616
R(V–O)/pm		
MRCI	195	159
CCSD	195	160
DFT	194	159
R(V–N)/pm		
MRCI	192	210
CCSD	192	211
DFT	186	210
R(N–O)/pm		
MRCI	125	357
CCSD	128	352
DFT	128	313
∠(NVO)/deg		
MRCI	37.6	149.9
CCSD	38.7	142.8
DFT	39.2	120.7
Q(V)/au		
MRCI	0.30	1.37
CCSD	0.35	1.27
DFT	0.48	1.06
Q(O)/au		
MRCI	−0.09	−0.73
CCSD	−0.13	−0.67
DFT	−0.18	−0.61
Q(N)/au		
MRCI	−0.21	−0.64
CCSD	−0.22	−0.60
DFT	−0.30	−0.45
ν(1, 2, 3)/cm^{-1}		
CCSD	461, 475, 1,236	128, 500, 1,000
DFT	458, 617, 1,237	157, 531, 1,048

would be extracting the nitrogen atom as soon as the initial activation barrier is overcome, i.e. a concerted substitution reaction. We have done calculations on the VON linear geometries by extracting the nitrogen atom, which resulted in passing through another transition state (TS3) with much higher energy than TS2 as can be seen in Fig. 1. As this pathway involves two potential barriers (AB and TS3) that are too high in comparison with the initial reactant energy, we think this direct concerted abstraction mechanism can be ruled out.

Table 3 Energy level (with respect to the V + NO) and geometrical parameters of the transition state connecting the V[NO] and NVO conformers (Step 2)

	MRCI	CCSD(T)	CCSD	DFT
ΔE/eV	0.460	0.469	0.804	0.055
R(V–N)/pm	196	CCSD	207	206
R(N–O)/pm	175	CCSD	170	164
∠(NVO)/deg	64.4	CCSD	59.0	59.4

The overall energy balance of the title reaction is difficult to calculate with accuracy because describing all steps of the reaction equitably even for this small system is somewhat beyond the present state of the art. When we use the available experimental data for the V–O bond energy, 6.458 eV [15], and the N–O bond energy, 6.497 eV [19], we obtain 0.039 eV of endothermicity. Our CCSD(T) gave 0.25 eV of endothermicity, which reflects the accuracy of the present treatment.

3.4 TS2 of the ScNO conformers

In our previous work on the Sc(^{2}D) + NO($^2\Pi_r$) → ScNO → ScO($^2\Sigma^+$) + N(^{4}S°) reaction [2], we could not locate the transition state connecting the two triangular conformers (TS2) of ScNO complex due to the divergence problem in the CCSD calculations. Using the basis set of the previous work, we were able to obtain TS2 this time. We report in Table 4 the energy levels of the minima and maxima involved in this reaction. Now TS2 is found well below the reactant energy level as was in the case of TiNO and TiO_2. The VNO case is quite different from other cases. The calculated activation barrier appears to be significantly higher than the experimental data, less than 0.10 eV [5, 6] as was the case with other reactions involving Ti and Sc, most likely due to the lack of the high-order electron correlation effect.

3.5 TS2 of the ScO_2 conformers

In our previous work on the Sc(^{2}D) + O_2($^3\Sigma_g^-$) → ScO_2 → ScO($^2\Sigma^+$) + O(^{3}P) reaction [2], we could not find the transition state connecting the two triangular conformers (TS2) of ScO_2 complex, either, due to the divergence problem in the CCSD calculations. We could obtain TS2 this time by the DFT method using the B3LYP functional. The energy level of TS2 is far below the reactant energy level, implying that the conversion of ScO_2 to OScO should intervene in the step equivalent to Step 2 for the monoxidation reaction of the scandium atom by the oxygen molecule to occur.

Table 4 Energy levels (in eV with respect to the Sc + NO) of the minima (conformers) and maxima (activation barrier, AB, and transition states, TS1 and TS2) involved in the $Sc(^2D) + NO(^2\Pi_r) \rightarrow ScO(^2\Sigma^+) + N(^4S°)$ reaction

	AB	Linear ScNO	TS1	Sc[NO]	TS2	NScO	Product
CCSD(T)	0.170	−0.942	−0.813	−1.965	−0.359	−2.397	−0.920
CCSD	0.214	−0.909	−0.544	−1.732	−0.110	−2.134	−0.681
DFT	None	−1.979	−1.583	−1.965	−0.867	−2.411	−0.324

4 Conclusion

In this paper, we have studied the potential energy surface for the oxidation reaction, $V(^4F) + NO(^2\Pi_r) \rightarrow VNO(^5A') \rightarrow VO(^4\Sigma^-) + N(^4S°)$, and the properties of the three VNO conformers. This work where we have used high-level methods to include electron correlation effects (CCSD, CCSD(T), and MRCI) combined with a large basis set suggests the activation energies much higher than the experiment. Calculating the reaction barrier of this small system remains a challenging problem of quantum chemistry as larger computational resources than we can afford today are required to perform a necessary large-scale correlated calculation. The DFT calculation using the B3LYP functional did not give any activation barrier at all, which is contrary to the experimental observations.

We present here the probable reaction mechanism passing through different maxima (transitions states, AB, TS1, TS2, and TS3) and minima (intermediates). The direct concerted substitution (abstraction) reaction through the VON linear geometry appears improbable because this process would have to overcome a high potential barrier (TS3).

Two stable conformers were found for the VNO intermediate, and the transition state connecting these conformers (TS2) appeared to be too high to consider any interconversion at low collision energy regime. This is in contrast to the TiNO and TiO_2 cases where this interconversion appeared to be possible. Our new calculation reported in this work showed the same feature for the ScNO complex and the ScO_2 complex with the energy level of the transition state connecting the two conformers below the reactant energy level. The relatively high transition state TS2 of the vanadium complex in comparison with the scandium and titanium complexes probably originates from the larger number of non-bonding electron in the former case. This work has also shown that the final step of the reaction (Step 3), the detachment of nitrogen atom, occurs without any potential barrier.

The effective point charges derived from the dipole moment indicate that a large electron transfer from the metal atom to the nitrogen and oxygen atoms occurs in the triangular NVO intermediate. In the other triangular conformer, V[NO], there is only a minor electron transfer from the metal atom to the NO moiety. Our work gave a fairly complete picture on the title reaction using the best and the largest computational methods available currently.

Acknowledgments This work was supported by grants (2009-0084918, 2010-0001632) from National Research Foundation, a national grant from KETEP of MKE, the EEWS program of KAIST, and CNRS. Computational resources were provided by the supercomputing center of the KISTI (KSC-2011-C2-18).

References

1. Ledentu V, Rahmouni A, Jeung GH, Lee YS (2004) Bull Korean Chem Soc 25:1645–1647
2. Kim KH, Lee YS, Kim D, Kim KS, Jeung GH (2002) J Phys Chem A 106:9600–9605
3. Kim KH, Lee YS, Moon JH, Kim Y, Jeung GH (2002) J Chem Phys 117:8385–8390
4. Naulin C, Costes M (1999) Chem Phys Lett 310:231–239
5. Luc P, Vetter R (2001) J Chem Phys 115:11106–11117
6. Jeung GH, Luc P, Vetter R, Kim KH, Lee YS (2002) Phys Chem Chem Phys 4:596–600
7. Naulin C, Hedgecock IM, Costes M (1997) Chem Phys Lett 266:335–341
8. Vetter R, Naulin C, Costes M (2000) Phys Chem Chem Phys 2:643–649
9. Ishida M, Yamashiro R, Matsumoto Y, Honma K (2006) J Chem Phys 124:204316-1–7
10. Karlström G, Lindh R, Malmqvist PÅ, Roos BO, Ryde U, Veryazov V, Widmark PO, Cossi M, Schimmelpfennig B, Neogrady P, Seijo L (2003) Comput Mater Sci 28:222–239
11. Werner HJ, Knowles PJ, Lindh R, Manby FR, Schütz M, and others (2006) MOLPRO, version 2006.1, a package of ab initio programs, see http://www.molpro.net
12. Frisch MJ, Trucks GW, Schlegel HB, Scuseria GE, Robb MA, Cheeseman JR, Montgomery JA, Vreven T, Kudin KN, Burant JC, Millam JM, Iyengar SS, Tomasi J, Barone V, Mennucci B, Cossi M, Scalmani G, Rega N, Petersson GA, Nakatsuji H, Hada M, Ehara M, Toyota K, Fukuda R, Hasegawa J, Ishida M, Nakajima T, Honda Y, Kitao O, Nakai H, Klene M, Li X, Knox JE, Hratchian HP, Cross JB, Bakken V, Adamo C, Jaramillo J, Gomperts R, Stratmann RE, Yazyev O, Austin AJ, Cammi R, Pomelli C, Ochterski JW, Ayala PY, Morokuma K, Voth GA, Salvador P, Dannenberg JJ, Zakrzewski VG, Dapprich S, Daniels AD, Strain MC, Farkas O, Malick DK, Rabuck AD, Raghavachari K, Foresman JB, Ortiz JV, Cui Q, Baboul AG, Clifford S, Cioslowski J, Stefanov BB, Liu G, Liashenko A, Piskorz P, Komaromi I, Martin RL, Fox DJ, Keith T, Al-Laham MA, Peng CY, Nanayakkara A, Challacombe M, Gill PMW, Johnson B, Chen W, Wong MW, Gonzalez C, Pople JA (2004) Gaussian 03, Revision C.02. Gaussian, Inc., Wallingford

13. Becke AD (1993) J Chem Phys 98:5648–5652
14. NIST Chemistry WebBook (2011) National Institute of Standards and Technology (NIST), Gaithersburg, MD. http://webbook.nist.gov/chemistry/. Accessed 8 Mar 2011
15. Pedley JB, Marshall EM (1983) J Phys Chem Ref Data 12:967–1031
16. Siegel MW, Celotta RJ, Hall JL, Levine J, Bennett RA (1972) Phys Rev A 6:607–631
17. Lee D, Lee YS, Hagebaum-Reignier D, Jeung GH (2006) Chem Phys 327:406–414
18. Jeung GH (2006) Theor Chem Acc 116:450–455
19. Huber KP, Herzberg G (1979) Molecular spectra and molecular structure IV. Constants of diatomic molecules. Van Nostrand Rheinhold, New York